Hollow Clay Brick Wall Propagation Analysis and Modified Brick Design for Enhanced Wi-Fi Coverage

David Ferreira, Rafael F. S. Caldeirinha, *Senior Member, IEEE*, Telmo R. Fernandes, *Senior Member, IEEE*, and Iñigo Cuiñas, *Senior Member, IEEE*

***Abstract*— The radiowave propagation through hollow clay brick walls, which are common in southern European construction, is analyzed. The brick walls have thicknesses of 11, 15, and 20 cm, common in both interior and exterior walls, and are bound with a portland cement, water, and sand mixture. For each brick dimension, three prototypes were assembled, varying in the type of wall finish, i.e., exposed brick, smooth painted plaster, and rough painted plaster. A 10 cm concrete wall was also included for comparison purposes. Penetration loss metrics were evaluated in an anechoic chamber at frequencies ranging from 680 MHz to 10 GHz. Results demonstrate that the brick wall internal heterogeneity, as well as the type of finish, significantly influences the propagation phenomena and thus the frequency response of the walls, with relatively high penetration losses observed at some relevant commercial frequency bands. Finally, an alternative brick design, with reduced penetration losses, is also proposed and evaluated under simulation environment only.**

***Index Terms*— Bricks, buildings, indoor radio communication, measurement, radio propagation, simulation.**

I. Introduction

WIRELESS communication systems are significantly influenced by the number and type of obstacles present in each deployment environment. The performance of such systems is often evaluated by implementing models, which may be categorized under three different types [1]–[4], such as empirical, statistical, and theoretical models. Some of these models describe obstacles on a macro-level through simple formulations, in an attempt to widen their applicability.

Manuscript received November 9, 2016; revised September 7, 2017; accepted October 28, 2017. Date of publication November 9, 2017; date of current version January 2, 2018. This work supported in part by the Portuguese Government, Foundation for Science and Technology, FCT, through the QREN-POPH funding, in part by the Spanish Government, Ministerio de Economía y Competitividad, Secretaría de Estado de Investigación, Desarrollo e Innovación, under Grant TEC2014-55735-C03-3R, in part by the AtlantTIC Research Center, and in part by the European Regional Development Fund. *(Corresponding author: Rafael F. S. Caldeirinha.)*

D. Ferreira is with the Instituto de Telecomunicações, 2411-901 Leiria, Portugal, and also with the Departamento de Teoría do Sinal e Comunicacións, Universidade de Vigo, 36310 Vigo, Spain.

R. F. S. Caldeirinha and T. R. Fernandes are with the Instituto de Telecomunicações, 2411-901 Leiria, Portugal, also with the School of Technology and Management, Polytechnic Institute of Leiria, 2411-901 Leiria, Portugal, and also with the School of Engineering, University of South Wales, Treforest CF37 1DL, U.K. (e-mail: rafael.caldeirinha@ipleiria.pt).

I. Cuiñas is with the Departamento de Teoría do Sinal e Comunicacións, Universidade de Vigo, 36310 Vigo, Spain.

Color versions of one or more of the figures in this paper are available online at http://ieeexplore.ieee.org.

Digital Object Identifier 10.1109/TAP.2017.2772028

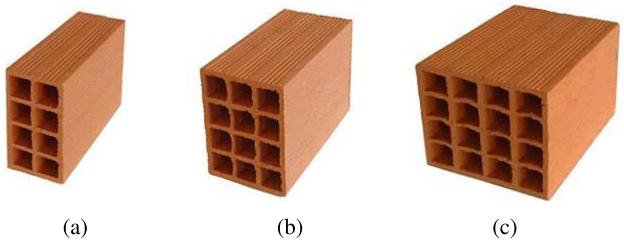

(a) (b) (c)

Fig. 1. Traditional bricks in southern European residential construction. (a) 11 cm. (b) 15 cm. (c) 20 cm.

European residential construction materials, more specifically for walls, are mostly based on clay bricks. In southern European countries, hollow bricks such as the ones in Fig. 1 are quite common in both interior and exterior walls. Other, more homogeneous materials, such as plasterboard, wood, concrete, or solid clay bricks, are also used in housing construction. The type of brick walls considered in this paper must be seen as the heterogeneous layers, as they exhibit a strong frequency-dependent response when exposed to a plane wave incident signal. This is associated with internal resonances within the wall, which are highly dependent on the brick internal arrangement, size, and orientation of the holes relative to wave polarization.

Most published work in the scientific literature mainly provides the dielectric parameters of bricks in order to describe their electromagnetic (EM) properties [5], [8]–[11], [14], or provide transmission coefficients which are directly related to the overall propagation losses across the material layer [6], [7], [12], [13]. As such, trying to characterize these objects by means of relative permittivity and loss tangent curves may not be an appropriate solution, resulting in rather linear propagation losses as a function of frequency. Fig. 2 shows simulated transmission values through walls with different materials, more specifically, a 11 cm solid brick (without holes), a 11 cm traditional brick, and a 10 cm concrete wall. This figure should provide the reader with the reasoning and relevance of this paper, in which the particular case of hollow clay bricks is yet to be properly studied and presented. With the advent of the Internet of Things (IoT) and other emerging

0018-926X © 2017 IEEE. Personal use is permitted, but republication/redistribution requires IEEE permission.
See http://www.ieee.org/publications_standards/publications/rights/index.html for more information.

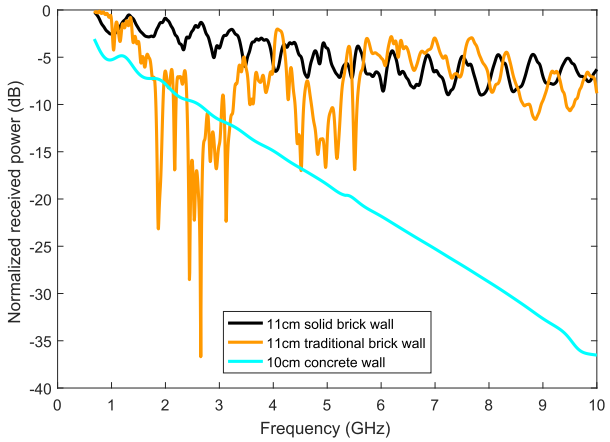

Fig. 2. Simulated transmission through different walls.

technologies, the indoor propagation characteristics through such layers is both timely and topical [15].

This paper is organized as follows. Section II provides a description of the type of bricks analyzed in this paper. In Section III, a detailed description of the measurement setup is provided. The most relevant measured results are also presented in this section. In Section IV, an alternative hollow clay brick design is proposed, with lower penetration losses at key commercial frequency bands. Finally, Section V draws the main conclusions of this paper.

II. Description of Studied Bricks

The hollow clay bricks, as shown in Fig. 1, follow standardized external dimensions of 290 mm × 190 mm (length × height) but with a set of width dimensions ranging from 40 to 220 mm, depending on the target application. For simplicity, these bricks are commonly referred to by their depth in centimeters. The square holes of each brick measure approximately 27 mm in side. For mechanical strengthening, the exterior walls typically employ two layers of brick masonry, with 11 and 15 cm brick spaced by an air gap and an insulation material [16], [17]. Internal walls may be composed of a layer of brick masonry (typically 11 cm bricks), or single/double layer of plasterboard [16], [17].

The experimental campaign devised to study the propagation loss due to traditional brick walls implied that several brick wall prototypes had to be built. Three different variants of hollow clay bricks were analyzed, namely, 11, 15, and 20 cm, assuming these to be the most common in residential construction in southern European countries. For each brick type, three wall prototypes were assembled for this study, each with a different finish layer, more specifically: rough painted plaster, smooth painted plaster, and bare brick. Fig. 3 shows such prototypes, among others, where all brick walls have been constructed placing the bricks in typical horizontal orientation. A 10 cm thick concrete wall sample was also manufactured for comparison purposes, due to its rather homogeneous properties. Fig. 3 also presents additional brick prototypes with paint only applied to a single side of the wall. All prototypes were assembled in an aluminum

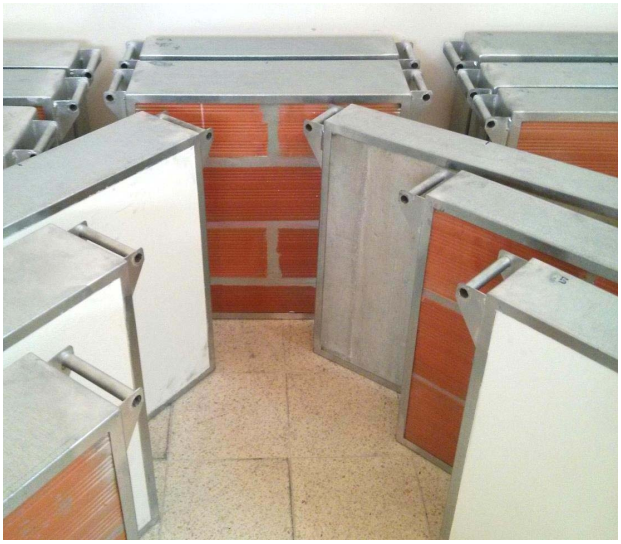

Fig. 3. Wall prototypes.

TABLE I
Measured Wall Variants

Wall sample #	Wall type	Wall finish
#1	Brick 11cm	None
#2	Brick 11cm	Smooth painted plaster
#3	Brick 11cm	Rough painted plaster
#4	Brick 15cm	None
#5	Brick 15cm	Smooth painted plaster
#6	Brick 15cm	Rough painted plaster
#7	Brick 20cm	None
#8	Concrete 10cm	None

casing to improve structural integrity and facilitate their movement and precise installation within the setup inside an anechoic chamber. The height and width of the casing are approximately 60 cm.

III. Measurement Setup, Results and Analysis

Penetration losses for all wall prototypes were measured, by means of a specific mechanical setup, inside an anechoic chamber. This section shows the idealized solution and presents the most relevant measurement results. Table I identifies the wall samples measured for this study, as well as the type of finish applied to both sides of the prototypes. A concrete wall sample was also manufactured for comparison purposes with the other samples.

A. Setup

The anechoic chamber setup consists of a mechanical test fixture whose dimensions are 1.8 m × 2 m (height × width), and its center was cut in a square shape with 45 cm × 45 cm. The structure is covered with pyramidal radio frequency (RF) absorbers and aluminum foil on one side, as illustrated in Fig. 4. The purpose of this fixture is to minimize the contamination of results due to diffraction and transmission mainly occurring through the center square window.

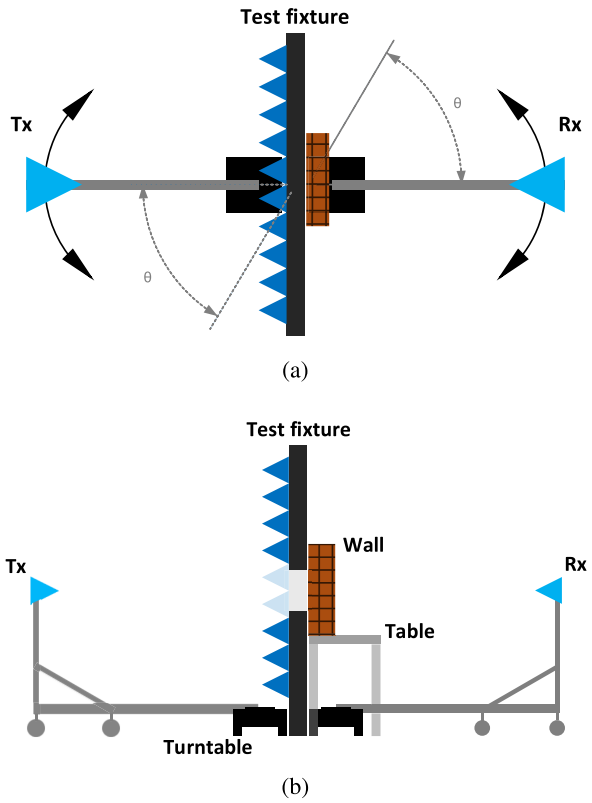

Fig. 4. Measurement setup geometry. (a) Top view. (b) Side view.

The antennas used in measurements were two identical wideband directional log-periodic antennas, connected to a vector network analyzer and placed on the top of rotating L-brackets. The antennas were rotated around the center of the fixture using a set of custom made mechanical rigs, actuated by computer controlled stepper motors. The repeatability of measurements and overall accuracy of the measurement system were determined to be less than 1 dB, ensuring the quality of the measurement data.

In order to determine the actual penetration losses associated with each wall sample, a free-space measurement was also required. This measurement, required for normalization purposes, was performed by keeping the test fixture in place and simply removing the presence of any wall sample from the support table.

Fig. 5 shows one of the wall prototypes under measurement from the transmitter end.

B. Normal Incidence

The results presented in this subsection have been normalized to a free-space measurement, therefore representing the actual penetration loss values.

Fig. 6 shows the results for the 11 cm brick wall samples under vertical polarization. From a quick observation, one may notice pronounced dips visible around the 2 GHz band. Second, the presence and type of wall finish does also appear to have an impact throughout the entire measured frequency range. Closely observing the 2 to 3 GHz band, a shift of the frequency null is apparent from the gathered results.

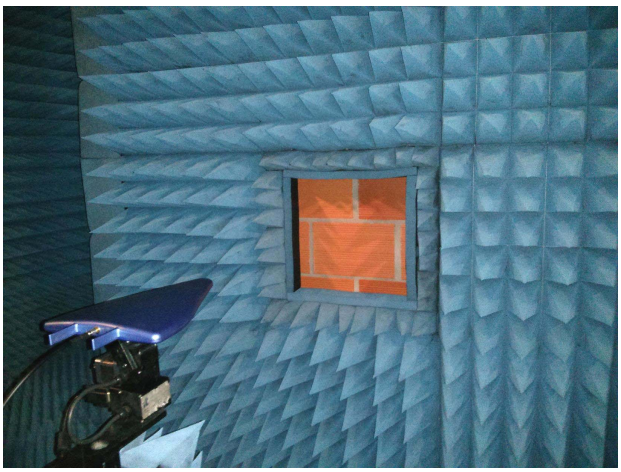

Fig. 5. Wall prototype under measurement.

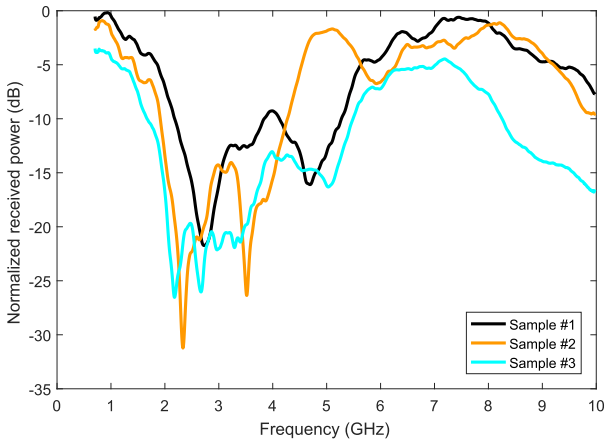

Fig. 6. Measurement results of the 11 cm brick wall samples, for vertical polarization.

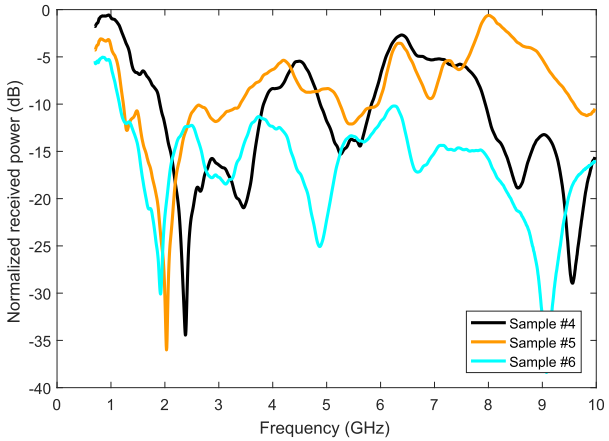

Fig. 7. Measurement results of the 15 cm brick wall samples, for vertical polarization.

The results obtained for the 15 cm brick wall samples present similar characteristics to the previous plot, as one may clearly observe from Fig. 7. More specifically, the frequency response is dependent on the type of finish applied to the facades, and the dips around the 2 GHz frequency mark also

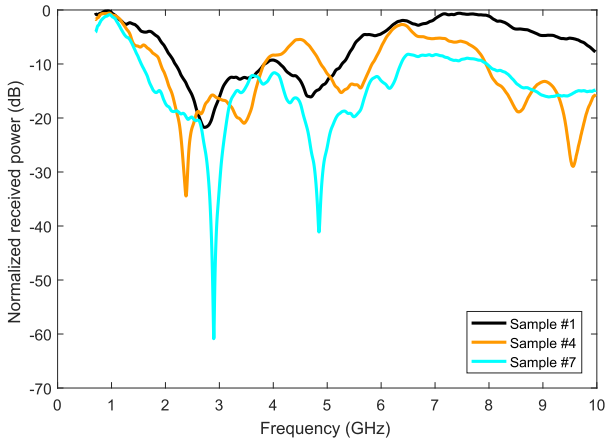

Fig. 8. Measurement results of the 11, 15, and 20 cm wall samples without plaster, for vertical polarization.

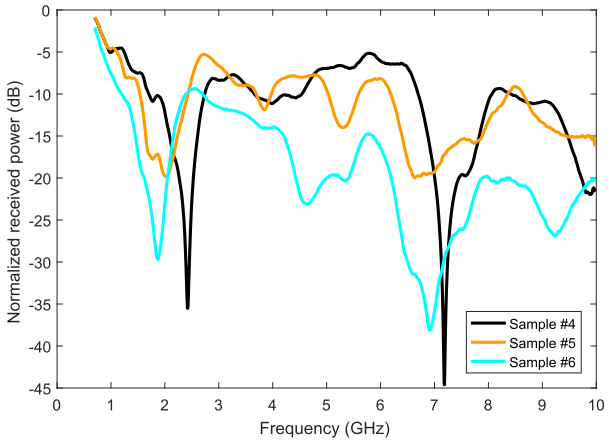

Fig. 10. Measurement results of the 15 cm brick wall samples, for horizontal polarization.

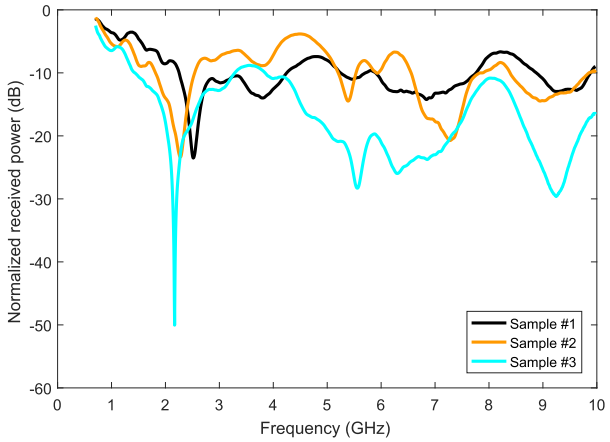

Fig. 9. Measurement results of the 11 cm brick wall samples, for horizontal polarization.

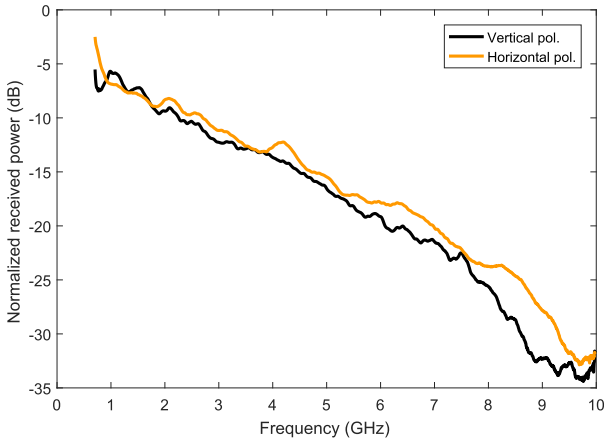

Fig. 11. Measurement results of a concrete wall (sample #8), for both main polarizations.

suffer a shift that seems to be associated with the type of wall finish.

In Fig. 8, frequency responses of bricks walls without plaster, i.e., samples #1, #4, and #7, are also presented. The transmission loss is more pronounced for the thicker brick walls. More pronounced dips are also visible for the 20 cm brick wall measurement.

Although slight manufacturing discrepancies could occur for all bricks used in this paper, and thus have impact on the measurement results, some conclusive observations may still be drawn. First, the type of brick used clearly has an impact on the transmission losses and on the presence and depth of frequency dips. Second, the type of finish appears to cause a frequency shift of the response, observable on the shifting of the transmission dips. Taking into consideration that the thickness of the finish layer is slightly different between smooth and rough painted plaster, such depth associated with specific dielectric parameters is, on the authors' opinion, responsible for the observed frequency offset of the transmission dips.

Figs. 9 and 10 illustrate the measurement results, in horizontal polarization, for the 11 and 15 cm wall samples, respectively. Significant differences may be observed in terms of resonant frequencies, despite the null depths being similar to those of the vertical polarization. This is mainly due to the alignment of the antenna polarization with the heterogeneous properties of the bricks' interior. More specifically, in the horizontal polarization case, the electric field was aligned with the brick internal holes.

To further highlight the difference between the transmission losses through homogeneous and heterogeneous walls, the measurement results for a concrete wall sample with 10 cm of thickness are shown in Fig. 11. This sample was produced at the same time as the brick wall samples, therefore sharing identical dimensions and within the same casing. The transmission response is relatively linear across the entire frequency range; therefore, the results substantially differ from those of the brick wall samples, and are in good agreement with simulations (see Fig. 2). Measurement results for horizontal and vertical polarizations yielded relatively similar behavior. However, one may still observe a significant penetration loss difference between both polarizations, particularly at 8.75 GHz with almost 6 dB between both curves. Such differences in amplitude, visible in the figure across the entire measurement frequency range, are not due to measurement system accuracy,

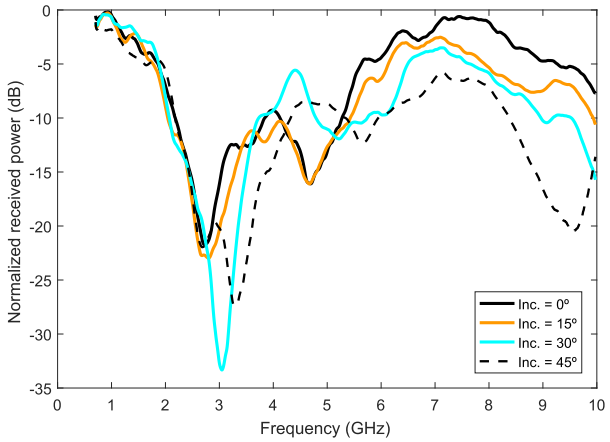

Fig. 12. Angular measurement results of the 11 cm brick wall sample without plaster (sample #1), for vertical polarization.

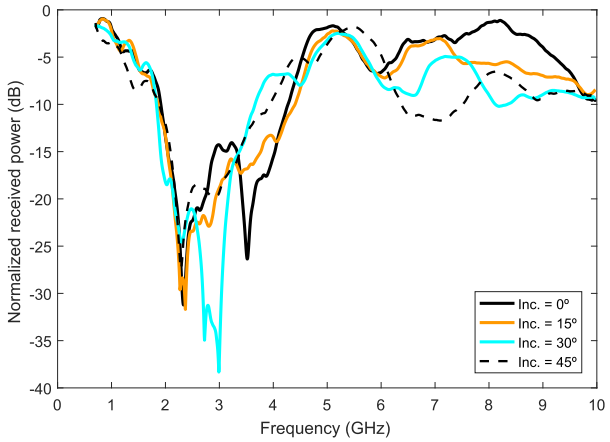

Fig. 13. Angular measurement results of the 11 cm brick wall sample with smooth plaster (sample #2), for vertical polarization.

but indeed attributed to the concrete sample. It may be concluded that the internal composition of the dried sample does still present some heterogeneity to incident RF signals, at these frequencies.

C. Angular Incidence

Figs. 12–15 demonstrate the angular transmission frequency response of brick wall samples #1, #2, #3, and #6, respectively. Despite the angular range data spanning from normal up to 45° in single degree steps, a step of 15° was used for displaying purposes. An incident angle-dependent transmission response is visible across all samples. From a close observation of the transmission dips present at normal incidence, one may notice a slight upward frequency offset of such dips with the increase in incidence angle.

D. Comparison With Simulation Model

At this point, the reader should have observed the considerable penetration losses of these brick walls at certain frequencies, which are substantially different than those of more homogeneous materials also used in residential construction,

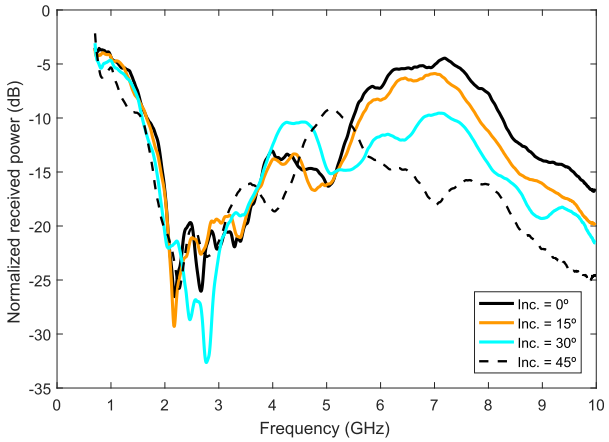

Fig. 14. Angular measurement results of the 11 cm brick wall sample with rough plaster (sample #3), for vertical polarization.

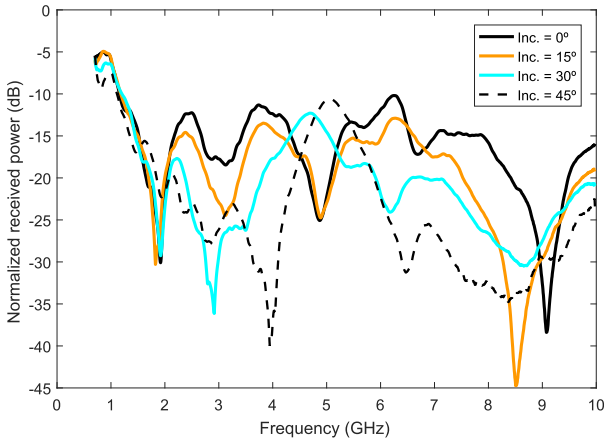

Fig. 15. Angular measurement results of the 15 cm brick wall sample with rough plaster (sample #6), for vertical polarization.

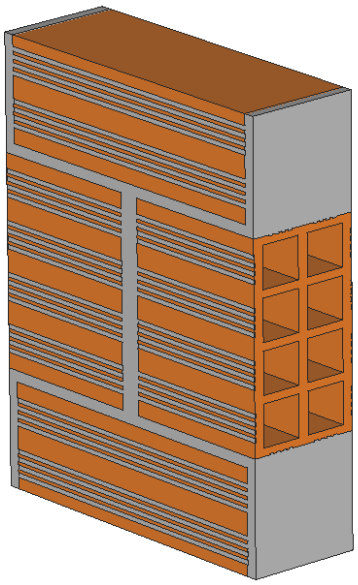

Fig. 16. Simulated brick wall unit cell, with 11 cm brick.

such as concrete, plasterboard, or wood. A model of a bare brick wall unit cell was developed in CST Microwave Studio Suite, as shown in Fig. 16, and simulated with a Floquet-mode

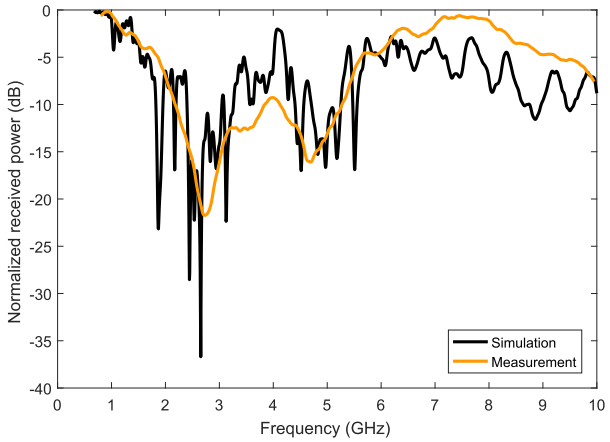

Fig. 17. Frequency response comparison, between simulation and measurement (#1) results for vertical polarization, of a brick wall composed of 11 cm brick, without plaster and paint.

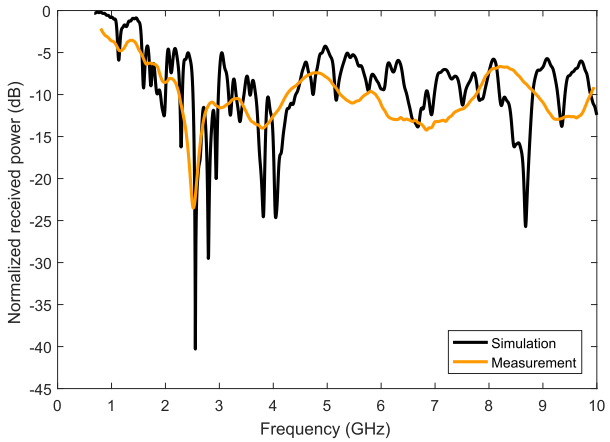

Fig. 18. Frequency response comparison, between simulation and measurement (#1) results for horizontal polarization, of a brick wall composed of 11 cm brick, without plaster and paint.

solver in frequency domain. The properties associated with the brick (represented in orange color) and binding cement (represented in gray color) were then adjusted to values within those mentioned in the literature. These values were subsequently slightly readjusted by comparison with measurement results, yielding some resemblance in the frequency response.

In Fig. 17, one may observe the simulation and measurement frequency curves of a 11 cm brick wall, without plaster or paint on the wall faces (equivalent to measured sample #1). In the simulation environment, the brick material was simulated with $\epsilon_r = 4.25$ and $\tan\delta = 0.01$, while the cement was defined with $\epsilon_r = 5.5$ and $\tan\delta = 0.05$. Both curves in the plot represent vertical polarization incidence, and perpendicular incidence with respect to the holes orientation. Fig. 18 provides a similar analysis, albeit for horizontal polarization. Both figures demonstrate a relatively good agreement, with pronounced transmission dips at various frequencies. Such effect is due to the bricks' specific internal arrangement and transitions between air and dielectric layers, more particularly, the comparable size of the holes with the incident signal quarter wavelength.

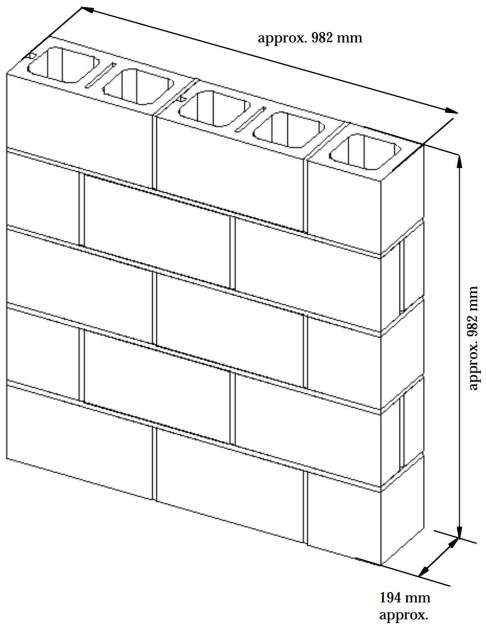

Fig. 19. Diagram of concrete masonry block wall, sample CB1 [13].

Due to the type of frequency response obtained from these heterogeneous brick walls, it is, in the authors' opinion, only reasonable to provide simple metrics, such as average penetration loss values as a function of frequency.

E. Comparison With Hollow Concrete Masonry Block

Stone [13] performed an extensive measurement campaign to assess the penetration loss values across several construction materials. Concrete masonry block walls were deemed appropriate for comparison with the hollow clay brick walls characterized in this paper. Contrary to the latter, the voids in the concrete masonry block walls run vertically and could also yield similar frequency response. To determine whether this was the case, hollow clay brick wall sample #7 was compared with a concrete masonry block wall computed from data present in [13], more specifically sample CB1, with a diagram shown in Fig. 19. The average dimensions of each concrete block in wall sample CB1 were 395 mm $\times$ 194 mm $\times$ 192 mm (length $\times$ width $\times$ height) [13]. Fig. 20 shows the results under vertical polarization.

From Fig. 20, the frequency response of the concrete masonry block wall is quite linear when compared with the 20 cm hollow clay brick wall. As such, and considering each concrete block measured almost 40 cm in length and only possesses two large square shaped voids averaging 12.5 cm in side, and one center void averaging 12.5 cm in width and 1 cm in length, one may deduce the size and number of voids of the hollow clay brick walls are indeed the main cause of such observed frequency response reported in this paper.

IV. Alternative Hollow Brick Design

In an attempt to improve the EM transparency, at least in the Wi-Fi frequency band, several approaches to the internal arrangement of the traditional 11 cm hollow brick were studied

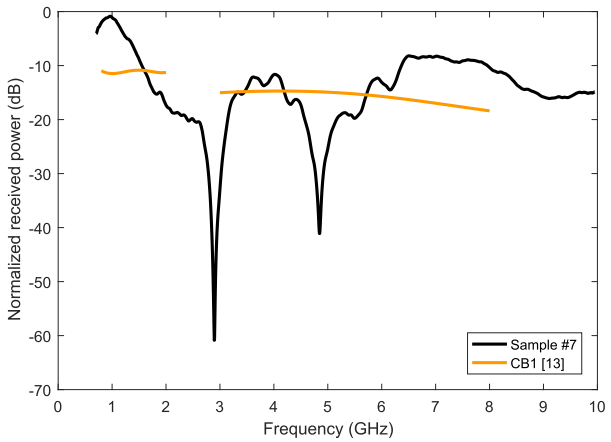

Fig. 20. Frequency response comparison between hollow clay brick wall sample #7, with 20 cm (CB1) concrete masonry block wall characterized in [13].

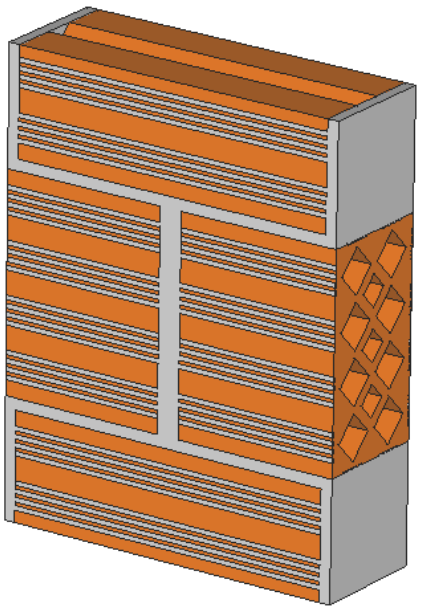

Fig. 21. Proposed alternative hollowed brick wall design for enhanced EM transmission at Wi-Fi frequency band. Four half bricks define the unit cell design.

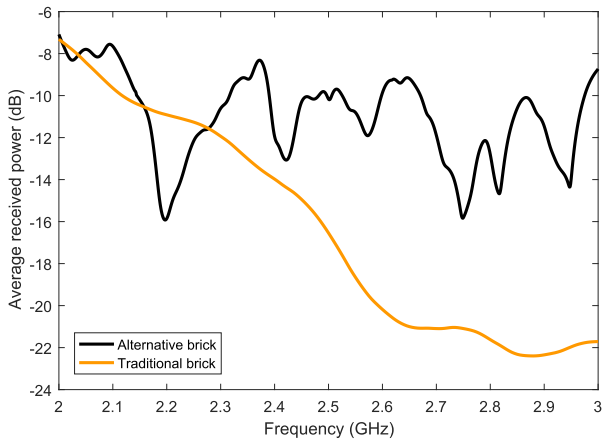

Fig. 22. Simulated average penetration gain comparison between the proposed brick and the traditional 11 cm hollowed clay brick, for angular range of 0° to 45° and for vertical polarization.

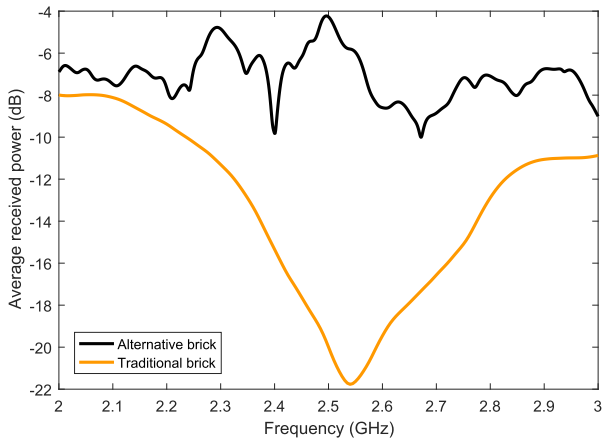

Fig. 23. Simulated average penetration gain comparison between the proposed brick and the traditional 11 cm hollowed clay brick, for angular range of 0° to 45° and for horizontal polarization.

and validated with the EM simulation tool. These included bricks with holes following geometric designs, such as square, hexagonal, and circular, followed by the inclusion of a third-middle row of holes with the same geometry. Focusing on transmission gains in both vertical and horizontal polarizations when compared with that of the traditional 11 cm brick, the brick wall unit cell design of Fig. 21 was obtained, with the brick and binding cement represented in orange and gray colors, respectively. The brick in this design has three rows of rectangular shaped cavities, rotated 45° in relation to the traditional design, where the top and bottom rows have a total of eight squares measuring 30 mm on their sides and the middle row has three 20 mm squares. It is assumed that the bricks have the cavities horizontally oriented when cemented into a wall and in the same plane as the wall, as is the case with the traditional bricks.

A relevant metric that should also be considered when comparing the proposed brick with the 11 cm traditional brick concerns the volume occupied by the holes. Each square shaped hole in the traditional bricks measures, approximately, 27 mm in side. Considering the 11 cm traditional brick, possessing eight holes, this equates to a total approximate "air" volume of 1690 cm^3. The proposed design has eight 30 mm holes and three 20 mm holes, equating a total of volume of 2440 cm^3. As such, the proposed brick should require slightly less volume of clay per brick, therefore reducing the manufacturing cost. The structural integrity of the proposed bricks to applied pressure, however, was not assessed and compared with the traditional ones.

The shaded gray volume in Fig. 21 represents the cement mixture bonding adjacent bricks in the wall. It is thought the particular arrangement of Fig. 21 minimizes, to an extent, the impact that internal resonances have on the overall frequency response at and around the Wi-Fi frequency band (due to equivalent dimensions compared with a quarter of the wavelength), therefore minimizing the observable transmission dips.

In order to better show the propagation benefits of this brick design, Figs. 22 and 23 have been included. The average penetration losses associated with both the proposed brick and

the traditional 11 cm brick, over an incidence angle range of 0° to 45°, in 5° steps, have been plotted for vertical and horizontal polarization incidences, respectively. The frequency range of these results was limited around the 2.4 GHz Wi-Fi band to better illustrate the expected transmission gains of the proposed brick design.

V. Conclusion

This paper presents a detailed analysis of the wireless propagation through hollow clay brick wall samples assembled according to traditional specifications within the European construction context, where significant penetration losses across a wide frequency range are observed. Such results are quite different from those obtained from solid bricks by other authors, which may compromise the applicability of well-established propagation models for path loss in indoor scenarios in the presence of hollow clay bricks.

An alternative brick design, with a different internal cavity arrangement was tailored and verified, through simulations, to yield significantly lower penetration losses at key commercial frequency bands. Gains of 10 dB on both main linear polarizations were attained at and around the Wi-Fi frequency band. The alternative bricks, by having less clay content per brick than traditional ones, should translate to slightly reduce manufacturing costs.

Overall, this paper highlights that wireless propagation through hollow clay brick walls should be considered in the world markets where these, and similar type of bricks, are commonly used in civil construction. Significant transmission losses were observed at frequency bands of interest, which may pose significant restrictions to both current and future commercial wireless communications, particularly in the context and for the scenarios of IoT.

References

[1] J. K. Tugnait and S. He, "Doubly-selective channel estimation using data-dependent superimposed training and exponential basis models," *IEEE Trans. Wireless Commun.*, vol. 6, no. 11, pp. 3877–3883, Nov. 2007.

[2] H. M. El-Sallabi, G. Liang, H. L. Bertoni, I. T. Rekanos, and P. Vainikainen, "Influence of diffraction coefficient and corner shape on ray prediction of power and delay spread in urban microcells," *IEEE Trans. Antennas Propag.*, vol. 50, no. 5, pp. 703–712, May 2002.

[3] J. K. Tugnait, S. He, and H. Kim, "Doubly selective channel estimation using exponential basis models and subblock tracking," *IEEE Trans. Signal Process.*, vol. 58, no. 3, pp. 1275–1289, Mar. 2010.

[4] N. R. Leonor, R. F. S. Caldeirinha, T. R. Fernandes, D. Ferreira, and M. G. Sánchez, "A 2D ray-tracing based model for micro- and millimeter-wave propagation through vegetation," *IEEE Trans. Antennas Propag.*, vol. 62, no. 12, pp. 6443–6453, Dec. 2014.

[5] A. V. Alejos, M. G. Sánchez, and I. Cuinas, "Measurement and analysis of propagation mechanisms at 40 GHz: Viability of site shielding forced by obstacles," *IEEE Trans. Veh. Technol.*, vol. 57, no. 6, pp. 3369–3380, Nov. 2008.

[6] N. W. Riley, D. J. Riley, and S. J. Yakura, "Grating lobes in RF propagation through brick and metal reinforced walls," in *Proc. IEEE Antennas Propag. Soc. Int. Symp.*, vol. 1A. Jul. 2005, pp. 367–370.

[7] O. A. Aziz and T. A. Rahman, "Comparison of indoor propagation models for multi floor staircase at 900 MHz and 1800 MHz," in *Proc. IEEE 2nd Int. Symp. Telecommun. Technol.*, Nov. 2014, pp. 174–178.

[8] I. Cuiñas and M. G. Sánchez, "Building material characterization from complex transmissivity measurements at 5.8 GHz," *IEEE Trans. Antennas Propag.*, vol. 48, no. 8, pp. 1269–1271, Aug. 2000.

[9] D. Ferreira, I. Cuiñas, R. F. S. Caldeirinha, and T. R. Fernandes, "A review on the electromagnetic characterisation of building materials at micro- and millimetre wave frequencies," in *Proc. Eur. Conf. Antennas Propag.*, 2014, pp. 145–149.

[10] S. Stavrou and S. R. Saunders, "Review of constitutive parameters of building materials," in *Proc. 12th Int. Conf. Antennas Propag.*, vol. 1. 2003, pp. 211–215.

[11] P. Protiva, J. Mrkvica, and J. Machác, "Estimation of wall parameters from time-delay-only through-wall radar measurements," *IEEE Trans. Antennas Propag.*, vol. 59, no. 11, pp. 4268–4278, Nov. 2011.

[12] N. R. Zulkefly, T. A. Rahman, A. M. Al-Samman, A. M. S. Mataria, and C. Y. Leow, "4G channel characterization for indoor environment at 2.6 GHz," in *Proc. IEEE 11th Int. Colloq. Signal Process. Appl.*, Mar. 2015, pp. 63–65.

[13] W. C. Stone, "Electromagnetic signal attenuation in construction materials," Building Fire Res. Lab., Nat. Inst. Standards Technol., Gaithersburg, MD, USA, Tech. Rep. 6055, Oct. 1997.

[14] F. Sagnard and G. El Zein, "*In situ* characterization of building materials for propagation modeling: Frequency and time responses," *IEEE Trans. Antennas Propag.*, vol. 53, no. 10, pp. 3166–3173, Oct. 2005.

[15] O. Hahm, E. Baccelli, H. Petersen, and N. Tsiftes, "Operating systems for low-end devices in the Internet of Things: A survey," *IEEE Internet Things J.*, vol. 3, no. 5, pp. 720–734, Oct. 2016.

[16] J. Mascarenhas, *Sistemas de Construção—II Paredes* (title in Portuguese). Lisbon, Portugal: Livros Horizonte, 2003.

[17] J. Mascarenhas, *Sistemas de Construção—III Paredes* (title in Portuguese). Lisbon, Portugal: Livros Horizonte, 2006.

[18] S. J. Orfanidis, "Electromagnetic waves and antennas," Ph.D. dissertation, Dept. Elect. Commun. Eng., Rutgers Univ., Piscataway, NJ, USA, 2016.

David Ferreira was born in Leiria, Portugal, in 1987. He received the Licenciatura and M.Sc. degrees in electrical and electronic engineering-telecommunications from the School of Technology and Management, Polytechnic Institute of Leiria, Leiria, in 2008 and 2010, respectively, and the Ph.D. degree in signal theory and communications from the Universidade de Vigo, Vigo, Spain, in 2017. His Ph.D. dissertation was in the radio frequency transparency control of building wall structures.

He is currently an RF Engineer at Blu Wireless Technology, Bristol, U.K.

Rafael F. S. Caldeirinha (M'00–SM'15) was born in Leiria, Portugal, in 1974. He received the B.Eng. degree (Hons.) in electronic and communication engineering and the Ph.D. degree in radiowave propagation from the University of Glamorgan, Trefforest, U.K., in 1997 and 2001, respectively. His Ph.D. dissertation was in vegetation studies at frequencies from 1 to 62.4 GHz.

He is currently the Head of the Antennas & Propagation Research Group with the Instituto de Telecomunicações, Leiria, and a Coordinator Professor in mobile communications with the School of Technology and Management, Polytechnic Institute of Leiria, Leiria. He has authored or co-authored over 110 papers in conferences and international journals and four contributions to ITU-R Study Group, which formed the basis of the ITU-R P.833-5 (2005) recommendation. His current research interests include the studies of radiowave propagation through vegetation media, radio channel sounding and modeling, and frequency selective surfaces, for applications at microwave and millimeter-wave frequencies.

Prof. Caldeirinha is a Fellow Member of IET. He is an Associate Editor of the IEEE Transactions on Antennas and Propagation journal and *IET on Microwaves, Antennas and Propagation* journal; a member of the Editorial Board of the *International Journal of Communication Systems*, (Wiley, New York); a Program Chair of the WINSYS International Conference from 2006 to 2012; an Appointed Officer for Awards and Recognitions of the IEEE Portugal Section in 2014; the Chair of the IEEE Portugal Joint Chapter on Antennas & Propagation, Electron Devices, and Microwave Theory & Techniques since 2016; and the Regional Delegate of the European Association for Antennas and Propagation for Andorra, Portugal, and Spain since 2017.

Telmo R. Fernandes (M'06–SM'16) was born in Coimbra, Portugal, in 1973. He received the Licenciatura degree in electrical engineering-telecommunications and electronics, the M.Sc. degree in electronic and telecommunication engineering from the University of Coimbra, Coimbra, in 1996 and 2000, respectively, and the Ph.D. degree in radio communication systems from the University of Glamorgan, Trefforest, U.K. His M.Sc. dissertation was titled Channel Assignment on Cellular Networks Using Neural Networks and Genetic Algorithms. His Ph.D. dissertation was in radiowave propagation modeling through vegetation at millimeter-wave frequencies.

In 1997, he joined the School of Technology and Management, Polytechnic Institute of Leiria, Leiria, Portugal, where he is currently an Adjunct Professor. From 2009 to 2011, he was the Head of the Electrical Engineering Department, and later in 2015, the coordinator of the electrical engineering M.Sc. course. He is currently a Researcher with the Antennas & Propagation Research Group, Instituto de Telecomunicações, Leiria. He has authored or co-authored over 70 scientific papers in international conferences and journals in the radiocommunications field.

Iñigo Cuiñas (M'08–SM'14) was born in Vigo, Spain, in 1971. He received the M.Eng. degree in telecommunication engineering and the Ph.D. degree from the Universidade de Vigo, Vigo, in 1996 and 2000, respectively.

He is a Professor with the Department of Signal Theory and Communications, Universidade de Vigo. He is currently the Dean of the School of Telecommunication Engineering, where he teaches courses on remote sensing and the social links of engineering. He has authored or co-authored over 70 papers in journals and 105 contributions to international conferences. His current research interests include radio wave propagation in complex environments, as vegetation media; the environmental aspects of radio frequency systems, as the development of techniques to reduce the electromagnetic pollution; and information security at physical level.

Prof. Cuiñas is a Reviewer of PROCEEDINGS OF THE IEEE, the IEEE TRANSACTIONS ON ANTENNAS AND PROPAGATION, the IEEE ANTENNAS AND WIRELESS PROPAGATION LETTERS, the *IEEE Antennas and Propagation Magazine*, the IEEE TRANSACTIONS ON VEHICULAR TECHNOLOGY, the IEEE TRANSACTIONS ON BROADCASTING, the *IEEE Communications Magazine*, *IET Electronics Letters*, *IET Microwaves, Antennas and Propagation*, *IET Communications*, *IET Sonar Radar and Navigation*, and several international conferences.